Astronomy & Astrophysics manuscript no. 19731
March 7, 2013

© ESO 2013

arXiv:1206.1177v2 [astro-ph.EP] 2 Oct 2012

WASP-78b and WASP-79b: Two highly-bloated hot Jupiter-mass exoplanets orbiting F-type stars in Eridanus [*]

B. Smalley[1], D. R. Anderson[1], A. Collier-Cameron[2], A. P. Doyle[1], A. Fumel[3], M. Gillon[3], C. Hellier,[1], E. Jehin[2], M. Lendl[4], P. F. L. Maxted[1], F. Pepe[4], D. Pollacco[5], D. Queloz[4], D. Ségransan[4], A. M. S. Smith[1], J. Southworth[1]
A. H. M. J. Triaud[4], S. Udry[4], R. G. West[6],

[1] Astrophysics Group, Keele University, Staffordshire, ST5 5BG, United Kingdom
e-mail: `b.smalley@keele.ac.uk`
[2] SUPA, School of Physics and Astronomy, University of St. Andrews, North Haugh, Fife, KY16 9SS, United Kingdom
[3] Université de Liège, Allée du 6 août 17, Sart Tilman, Liège 1, Belgium
[4] Observatoire de Genève, Université de Genève, Chemin des maillettes 51, 1290 Sauverny, Switzerland
[5] Astrophysics Research Centre, School of Mathematics & Physics, Queen's University Belfast, University Road, Belfast BT7 1NN, United Kingdom
[6] Department of Physics and Astronomy, University of Leicester, Leicester, LE1 7RH, United Kingdom

Received ¡date¿ / accepted ¡date¿

ABSTRACT

We report the discovery of WASP-78b and WASP-79b, two highly-bloated Jupiter-mass exoplanets orbiting F-type host stars. WASP-78b orbits its $V = 12.0$ host star (TYC 5889-271-1) every 2.175 days and WASP-79b orbits its $V = 10.1$ host star (CD-30 1812) every 3.662 days. Planetary parameters have been determined using a simultaneous fit to WASP and TRAPPIST transit photometry and CORALIE radial-velocity measurements. For WASP-78b a planetary mass of $0.89 \pm 0.08\ M_{\rm Jup}$ and a radius of $1.70 \pm 0.11\ R_{\rm Jup}$ is found. The planetary equilibrium temperature of $T_{\rm P} = 2350 \pm 80$ K for WASP-78b makes it one of the hottest of the currently known exoplanets. WASP-79b its found to have a planetary mass of $0.90 \pm 0.08\ M_{\rm Jup}$, but with a somewhat uncertain radius due to lack of sufficient TRAPPIST photometry. The planetary radius is at least $1.70 \pm 0.11\ R_{\rm Jup}$, but could be as large as $2.09 \pm 0.14\ R_{\rm Jup}$, which would make WASP-79b the largest known exoplanet.

Key words. planets and satellites: general – stars: individual: WASP-78 – stars: individual: WASP-79 – techniques: photometry – techniques: spectroscopy – techniques: radial velocities

1. Introduction

The first exoplanets were discovered using the radial velocity technique (Mayor & Queloz 1995). However, following the detection of a transiting exoplanet (Charbonneau et al. 2000), several ground-based and space-based survey projects have dramatically increased the number of known systems. Transiting exoplanets allow parameters such as the mass, radius, and density to be precisely determined, as well as their atmospheric properties to be studied during their transits and occultations (Charbonneau et al. 2005; Southworth 2009; Winn 2009).

Most of the transiting exoplanets found by ground-based surveys are 'hot Jupiters', with orbital periods of up to around 5 days. Many of these have radii larger than predicted by irradiated planet models (Fortney et al. 2007). Several have markedly low densities, with WASP-17b (Anderson et al. 2010, 2011), Kepler-12b (Fortney et al. 2011) and Kepler-7b (Latham et al. 2010) having a density less than 1/10 that of Jupiter. The mechanisms for producing such bloated planets are at present unclear (Fortney & Nettelmann 2010), but several have been proposed, including Ohmic heating in the planetary atmosphere (Batygin & Stevenson 2010; Perna et al. 2010) and thermal tidal effects (Arras & Socrates 2010).

In this paper we report the detection of WASP-78b and WASP-79b, two highly-bloated Jupiter-mass planets in orbit around F-type stars. We present the WASP-South discovery photometry, together with follow-up optical photometry and radial velocity measurements.

2. WASP-South photometry

The WASP project has two robotic observatories; one on La Palma in the Canary Islands and another in Sutherland in South Africa. The wide angle survey is designed to find planets around relatively bright stars in the V-magnitude range $9 \sim 13$. A detailed description is given in Pollacco et al. (2006).

The pipeline-processed data were de-trended and searched for transits using the methods described in Collier Cameron et al. (2006), yielding detections of periodic, transit-like signatures on two stars in the constellation Eridanus (Fig. 1). The $V = 12.0$ star WASP-78 (1SWASPJ041501.50-220659.0; TYC 5889-271-1) exhibited $\sim$0.010 mag. transits every 2.175 days, while the $V = 10.1$ star WASP-79 (1SWASPJ042529.01-303601.5; CD-30 1812) showed $\sim$0.015 mag. transits every 3.66 days. A total of 16489 observations of WASP-78 were obtained between 2006 August and 2009 December and 15424 observations of WASP-79 were obtained between 2006 September and 2010 February.

---

[*] Radial velocity and photometric data are only available in electronic form at the CDS via anonymous ftp to `cdsarc.u-strasbg.fr (130.79.128.5)` or via http://cdsarc.u-strasbg.fr/viz-bin/qcat?J/A+A/???/A??

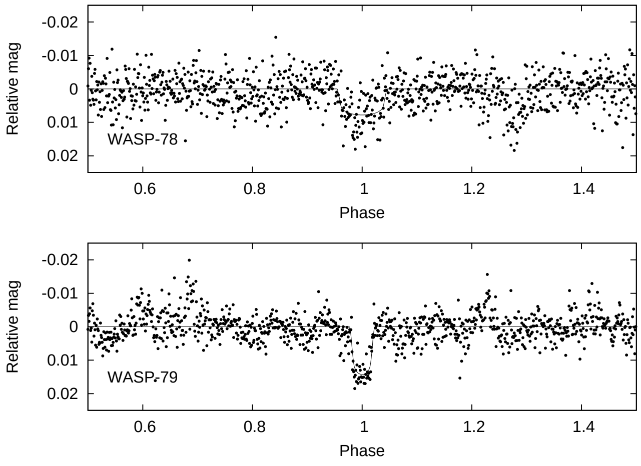

Fig. 1. WASP photometry of WASP-78 and WASP-79 folded on the best-fitting orbital periods and binned into phase bins of 0.001. The solid line is the model fit presented in Sect. 6.

There is a 15th mag. star, 2MASS 04150416-2207189, located 42″ away from WASP-78, which is just within the photometric extraction aperture. However, the dilution is only 2% and does not significantly affect the depth of the WASP transits. Around 24″ away from WASP-79, is 6dFGS gJ042530.8-303554, a 16th mag. redshift $z = 0.069$ galaxy (Jones et al. 2009). This is, however, too faint to significantly dilute the WASP-79 photometry. The spectral type of WASP-79 is listed as F2 in Jackson & Stoy (1954).

3. Spectroscopic observations with CORALIE

Spectroscopic observations were obtained with the CORALIE spectrograph on the Swiss 1.2m telescope. The data were processed using the standard pipeline (Baranne et al. 1996; Queloz et al. 2000; Pepe et al. 2002). A total of 17 and 21 radial velocity (RV) and line bisector span ($V_{\rm span}$) measurements were made for WASP-78 and WASP-79, from 2011 October 09 to 2011 December 30, and 2010 December 12 to 2012 February 07, respectively (Table 1). The bisector spans are a measure of the asymmetry of the cross-correlation function and, based on our experience, have standard errors of $\approx 2\sigma_{\rm RV}$.

The amplitude of the RV variations and the absence of any correlation with orbital phase of the line bisector spans ($V_{\rm span}$) in Fig. 2 indicates that it is highly improbable that the RV variations are due to an unresolved eclipsing binary or chromospheric activity (Queloz et al. 2001).

In the case of WASP-79 one RV point (HJD 2455874.830894) was taken during transit. This is affected by the Rossiter-McLaughlin effect and has been excluded from the fitting process.

4. TRAPPIST photometry

Photometric observations of transits were obtained using the 60cm robotic TRAPPIST Telescope (Gillon et al. 2011a,b; Jehin et al. 2011). Since the telescope has a German equatorial mount, there are short gaps in the lightcurves at the times of culmination due to meridian flips, when the telescope is reversed to the other side the pier.

Table 1. Radial velocity (RV) and line bisector spans ($V_{\rm span}$) measurements for WASP-78 and WASP-79 obtained by CORALIE spectra.

BJD–2 400 000 (UTC)	RV (km s^{-1})	$V_{\rm span}$ (km s^{-1})
	WASP-78	
55843.80914	0.3565 ± 0.0349	+0.0443
55844.85276	0.6078 ± 0.0404	+0.2036
55856.82996	0.3477 ± 0.0388	−0.0086
55858.75524	0.3932 ± 0.0409	+0.0772
55859.84448	0.5282 ± 0.0339	+0.1423
55863.77620	0.4233 ± 0.0281	+0.1274
55864.77388	0.5390 ± 0.0284	+0.1252
55868.78606	0.5463 ± 0.0320	+0.1018
55872.82630	0.5131 ± 0.0346	−0.1311
55880.77994	0.3302 ± 0.0240	+0.1064
55881.82771	0.5734 ± 0.0272	+0.0760
55883.69133	0.5093 ± 0.0260	+0.1505
55887.76423	0.4160 ± 0.0231	+0.0627
55888.64129	0.5431 ± 0.0281	+0.0722
55889.62002	0.3780 ± 0.0257	+0.0949
55894.74373	0.5875 ± 0.0238	+0.0426
55925.58825	0.5346 ± 0.0206	+0.0972
	WASP-79	
55542.63132	4.8915 ± 0.0260	−0.2869
55573.65244	5.1141 ± 0.0225	−0.1877
55595.61945	5.0768 ± 0.0267	−0.2985
55832.81511	4.9912 ± 0.0280	−0.3792
55856.85501	4.9258 ± 0.0319	−0.2776
55858.83490	4.9823 ± 0.0315	−0.1275
55863.73949	4.9772 ± 0.0232	−0.2613
55864.82478	4.8688 ± 0.0236	−0.2901
55865.67114	4.9591 ± 0.0282	−0.3785
55867.86163	4.9566 ± 0.0241	−0.2958
55868.67269	4.9228 ± 0.0267	−0.2961
55869.70268	5.0298 ± 0.0266	−0.2612
55870.84257	5.0119 ± 0.0249	−0.2504
55871.79821	4.9102 ± 0.0249	−0.3420
55872.78874	4.9724 ± 0.0251	−0.3896
55873.83187	5.0848 ± 0.0260	−0.3053
55874.83089	5.1331 ± 0.0486	−0.6088
55883.76896	4.9481 ± 0.0252	−0.2040
55886.77560	4.9336 ± 0.0300	−0.3774
55888.67590	5.0633 ± 0.0258	−0.1902
55925.65354	5.0572 ± 0.0200	−0.2109
55964.62745	5.0409 ± 0.0216	−0.3219

4.1. WASP-78b

A total of three transits of WASP-78b were observed with TRAPPIST. The observations were made through a ‘blue-blocking’ filter with a transmittance >90% above 500nm. The exposure times were 15s and the telescope was defocused, the mean FWHM being 5 pixels (pixel scale = 0.65″).

The first transit was observed on 2011 November 8 from 01h23 to 08h00 UTC. The first ≈75% of the run was slightly cloudy. There was a meridian flip at HJD 2455873.748. The resulting lightcurve has 949 measurements.

A second transit was observed on 2011 December 15 from 00h23 to 06h44 UTC. Transparency was good this time. A meridian flip occurred at HJD 2455910.646. The resulting lightcurve has 918 measurements.

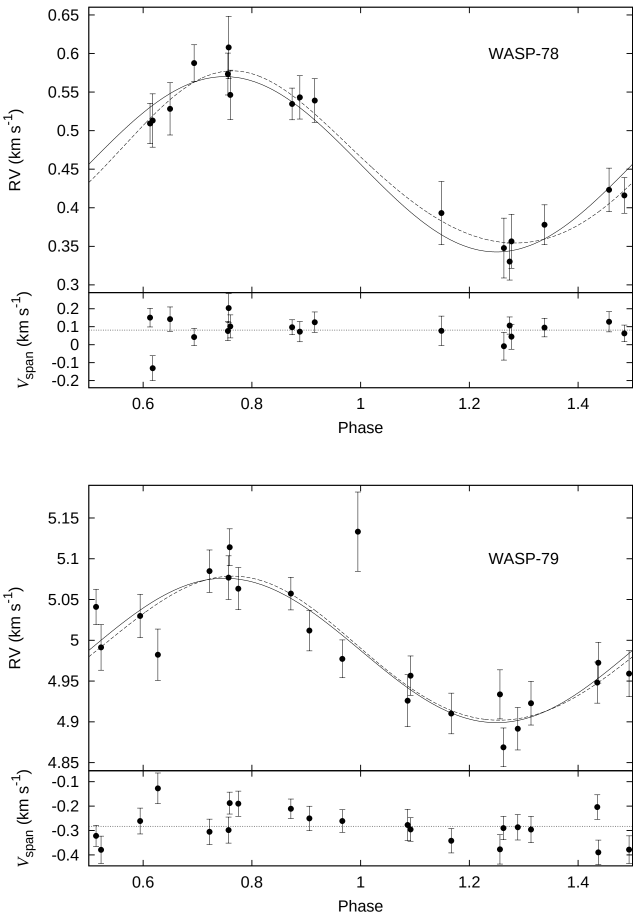

Fig. 2. Radial velocity variations and line bisectors ($V_{\rm span}$) of WASP-78 and WASP-79 folded on the best-fitting circular orbit periods (solid lines). The eccentric orbit solutions are shown as dashed-lines (See Sect. 6 for discussion). The bisector uncertainties of twice the RV uncertainties have been adopted. The mean values of the bisectors are indicated by the dotted lines. There is negligible correlation between $V_{\rm span}$ and orbital phase.

The third transit was observed on 2012 January 8 from 00h45 to 05h30 UTC. However, only part of the transit was observed. Transparency was good. A meridian flip occurred at HJD 2455934.579. The resulting lightcurve has 697 measurements.

4.2. WASP-79b

For WASP-79b only a partial transit was observed with TRAPPIST on 2011 September 26 from 07:33 to 09:52 UTC. It was obtained in z' band. The exposure times were 20s and the telescope was defocused by 300 focuser steps with the mean FWHM being 5 pixels. The sky conditions were good. Due to a software problem, there is a gap of a few minutes in the first half of the lightcurve. There was a meridian flip at HJD 2455830.870. The resulting lightcurve has 244 measurements.

5. Spectral Analysis

The individual CORALIE spectra of WASP-78 and WASP-79 were co-added to produce spectra with average S/N of around 50:1 and 90:1, respectively. The standard pipeline reduction products were used in the analysis. The analysis was performed using the methods given in Gillon et al. (2009). The km s^{-1} and H_β lines were used to determine the effective temperature ($T_{\rm eff}$). The surface gravity ($\log g$) was determined from the Ca i lines at 6162Å and 6439Å (Bruntt et al. 2010a), along with the Na i D lines. The Na D lines are affected by weak interstellar absorption. For WASP-78 this is around 40mÅ, while for WASP-79 it is only around 10mÅ. However, in both cases it is possible to fit the blue wings which are unaffected by the interstellar lines. The elemental abundances were determined from equivalent width measurements of several clean and unblended lines. A value for microturbulence ($\xi_{\rm t}$) was determined from Fe i using the method of Magain (1984). The ionization balance between Fe i and Fe ii and the null-dependence of abundance on excitation potential were used as an additional the $T_{\rm eff}$ and $\log g$ diagnostics (Smalley 2005). The parameters obtained from the analysis are listed in Table 2. The quoted error estimates include that given by the uncertainties in $T_{\rm eff}$, $\log g$ and $\xi_{\rm t}$, as well as the scatter due to measurement and atomic data uncertainties. Also given are estimated masses and radii using the Torres et al. (2010) calibration. These values, however, are not using in determining the planetary parameters, since $T_{\rm eff}$ and [Fe/H] are the only stellar input parameters (see Sect. 6).

5.1. WASP-78

There is no significant detection of lithium in the spectrum, with an equivalent width upper limit of 4mÅ, corresponding to an abundance of $\log A({\rm Li}) < 0.71 \pm 0.12$. This implies an age of at least several Gyr (Sestito & Randich 2005). A rotation rate of $P = 10.5 \pm 2.4$ d is implied by the $v \sin i_\star$. This gives a gyrochronological age of $\sim 1.37^{+1.91}_{-0.78}$ Gyr using the Barnes (2007) relation.

5.2. WASP-79

There is lithium in the spectra, with an equivalent width of 8±1 mÅ, corresponding to an abundance of $\log A({\rm Li}) = 1.94 \pm 0.07$. The lithium abundance of WASP-79 is an ineffective age constraint because of the high effective temperature of this star. In addition, the star is close to the lithium gap where depletion occurs in the 0.6 Gyr-old Hyades (Boesgaard & Tripicco 1986; Böhm-Vitense 2004). A rotation rate of $P = 4.0 \pm 0.8$ d is implied by the $v \sin i_\star$. This gives a gyrochronological age of at least $\sim$ 0.5 Gyr using the Barnes (2007) relation. However, gyrochronology does not provide a reliable age constraint for such a hot star.

6. Planetary system parameters

To determine the planetary and orbital parameters, a simultaneous fit the CORALIE radial velocity measurements and both the WASP and TRAPPIST photometry was performed, using the Markov Chain Monte Carlo (MCMC) technique. The details of this process are described in Collier Cameron et al. (2007) and Pollacco et al. (2008). Four sets of solutions were used: with and without the main-sequence mass-radius constraint (which imposes a Gaussian prior on the stellar radius using a mass-radius relation $R_\star = M_\star^{0.8}$ with $\sigma_R = 0.1R$.) for both circular and floating eccentricity orbits. Limb-darkening uses the four-coefficient model of Claret (2000) and vary with any change in $T_{\rm eff}$ during the MCMC fitting process. For WASP data and TRAPPIST with blue-blocking filter the R-band is used. The final values of the limb-darkening coefficients are noted in Tables 3 and 4.

Table 2. Stellar parameters of WASP-78 and WASP-79

Parameter	WASP-78	WASP-79
Star	TYC 5889-271-1	CD-30 1812
RA (J2000)	04h 15m 01.50s	04h 25m 29.01s
Dec (J2000)	$-22°06'59.0''$	$-30°36'01.5''$
V mag.	12.0	10.1
$T_{\rm eff}$	6100 ± 150 K	6600 ± 100 K
$\log g$	4.10 ± 0.20	4.20 ± 0.15
$\xi_{\rm t}$	1.1 ± 0.2 km s^{-1}	1.3 ± 0.1 km s^{-1}
$v_{\rm mac}$	3.5 ± 0.3 km s^{-1}	6.4 ± 0.3 km s^{-1}
$v \sin i_\star$	7.2 ± 0.8 km s^{-1}	19.1 ± 0.7 km s^{-1}
[Fe/H]	−0.35 ± 0.14	+0.03 ± 0.10
[Si/H]	−0.25 ± 0.09	+0.06 ± 0.08
[Ca/H]	−0.14 ± 0.14	+0.25 ± 0.14
[Ti/H]	−0.02 ± 0.08	...
[Cr/H]	...	+0.04 ± 0.19
[Ni/H]	−0.42 ± 0.10	−0.06 ± 0.10
$\log A$(Li)	< 0.71 ± 0.12	1.94 ± 0.07
Mass	1.17 ± 0.13 $M_\odot$	1.38 ± 0.12 $M_\odot$
Radius	1.60 ± 0.41 $R_\odot$	1.53 ± 0.31 $R_\odot$
Spectral Type	F8	F5
Distance	550 ± 120 pc	240 ± 50 pc

Notes. Values of mactroturbulence ($v_{\rm mac}$) are based on the calibration by Bruntt et al. (2010). Mass and radius are estimated using the Torres et al. (2010) calibration. The spectral types are estimated from $T_{\rm eff}$ using Table B.1 in Gray (2008).

A value of the stellar mass determined as part of the MCMC process, uses the empirical calibration of Southworth (2009) in which mass is estimated as a function of $T_{\rm eff}$, [Fe/H] and stellar density ($\rho_\star$). The uncertainty in the derived stellar mass is dominated by the uncertainties in the spectroscopic values of $T_{\rm eff}$ and [Fe/H]. At each step in the Markov chain, these quantities are given random gaussian perturbations, and controlled by priors assuming gaussian random errors in the spectroscopic values. The stellar density is derived at each step in the chain from the scaled stellar radius $R_\star/a$ and the impact parameter (b). The uncertainty in the stellar mass is computed directly from the posterior probability distribution, and takes the uncertainties in $T_{\rm eff}$, [Fe/H] and $\rho_\star$ fully into account. The posterior probability distribution for the stellar radius follows from the mass and density values at each step in the chain.

6.1. WASP-78b

The spectroscopic analysis suggests that WASP-78 might be slightly evolved. In addition, we have three TRAPPIST lightcurves, which allows for the main-sequence constraint to be removed (Fig. 3). The rms of the fits to the TRAPPIST lightcurves is 2.33 mmag., which is no better than that obtained with the main-sequence constraint applied. However, the main-sequence constraint forces the fitting process to a higher stellar mass (2.0 $M_\odot$), higher $T_{\rm eff}$ (6640 K) and low impact parameter (0.06), whilst still finding a large stellar radius (2.3 $R_\odot$) and, hence, planetary radius (1.75 $R_{\rm Jup}$). Such a high values stellar mass and $T_{\rm eff}$ are inconsistent with the spectroscopic analysis of the host star. Furthermore, fixing $T_{\rm eff}$ and [Fe/H] to their spectroscopic values yields a slightly worse main-sequence-constrained fit to the photometry.

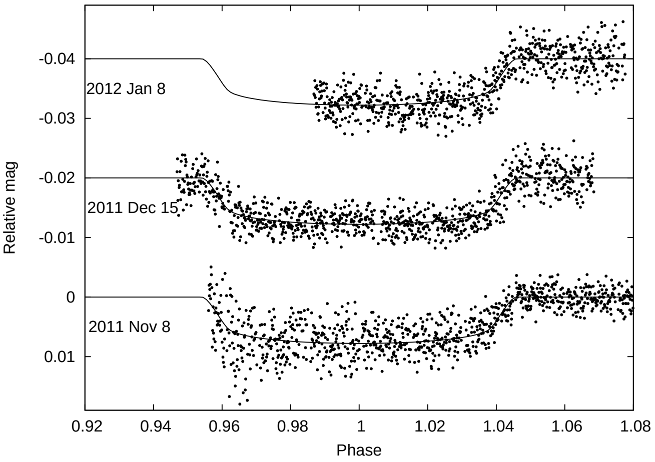

Fig. 3. TRAPPIST transits of WASP-78b. The solid-line is the model fit presented in Sect. 6. The lightcurves are offset for clarity.

Table 3. System parameters for WASP-78b.

Parameter	Value
Transit epoch (HJD, UTC), T_0	2455882.35878 ± 0.00053
Orbital period, P	2.17517632 ± 0.0000047 d
Transit duration, T_{14}	0.1953 ± 0.0013 d
Transit depth, $(R_{\rm P}/R_*)^2$	0.0063 ± 0.0002
Impact parameter, b	$0.417\,^{+0.079}_{-0.129}$
Stellar reflex velocity, K_1	0.1136 ± 0.0096 km s^{-1}
Centre-of-mass velocity at time T_0, γ	0.4564 ± 0.0020 km s^{-1}
Orbital separation, a	0.0362 ± 0.0008 AU
Orbital inclination, i	$83.2\,^{+2.3}_{-1.6}$ °
Orbital eccentricity, e	0.0 (assumed)
Stellar density, $\rho_\star$	0.125 ± 0.018 $\rho_\odot$
Stellar mass, $M_\star$	1.33 ± 0.09 $M_\odot$
Stellar radius, $R_\star$	2.20 ± 0.12 $R_\odot$
Stellar surface gravity, $\log g_\star$	3.88 ± 0.04
Planet mass, $M_{\rm P}$	0.89 ± 0.08 $M_{\rm Jup}$
Planet radius, $R_{\rm P}$	1.70 ± 0.11 $R_{\rm Jup}$
Planet surface gravity, $\log g_{\rm P}$	2.84 ± 0.06
Planet density, $\rho_{\rm P}$	0.18 ± 0.04 $\rho_{\rm Jup}$
Planet equilibrium temperature, $T_{\rm P}$	2350 ± 80 K

Notes. The planet equilibrium temperature, $T_{\rm P}$, assumes a Bond albedo of $A = 0$ and even redistribution of heat around the planet. Limb-darkening coefficients were $a1 = 0.388$, $a2 = 0.609$, $a3 = -0.395$ and $a4 = 0.075$

With the eccentricity floating, a value of $e = 0.078^{+0.054}_{-0.049}$ is found. This fit has a $\chi^2 = 6.04$, compared to $\chi^2 = 7.92$ for a circular orbit. Using the Lucy & Sweeney (1971, Eq. 27) F-test shows that there is a 17.2% probability that the improvement could have arisen by chance. This is too high to confidently claim detection of eccentricity. Thus, we present the system parameters for the circular-orbit solutions (Table 3), but note that the 3-σ upper limit on eccentricity is 0.24. Anderson et al. (2012) presented a discussion on the justification of adoption of circular orbit in these cases. Further RV measurements, or occultation photometry, are required to constrain the possible eccentricity of the system.

6.2. WASP-79b

With the eccentricity floating, a value of $e = 0.035^{+0.044}_{-0.024}$ is found with a $\chi^2 = 20.9$, which is not significantly lower than $\chi^2 = 21.0$ for a circular orbit. Hence, there is no evidence for any orbital eccentricity in the current RV data. Hence, we adopt a circular orbit for WASP-79b.

There is only a single partial TRAPPIST light curve and there are insufficient points before ingress to reliably determine the out-of-transit level (Fig. 4). The non-main-sequence constrained solution gives an rms of 1.62 mmag. for the TRAPPIST photometry alone, compared to a slightly larger value of 1.69 mmag. for that with the main-sequence constraint applied. In addition, the main-sequence constraint has forced the fitting to a slightly higher $T_{\rm eff}$ (6660 K) and [Fe/H] (+0.24) than found from the spectroscopy. Fixing $T_{\rm eff}$ and [Fe/H] to their spectroscopic values produces a slightly worse fit. The WASP photometry shows the depth is well determined, but is unable help in constraining the shape and duration of the ingress and egress. Thus, we present both the main-sequence and non-main-sequence constrained circular orbit solutions in Table 4 and discuss them further in Sect. 7.

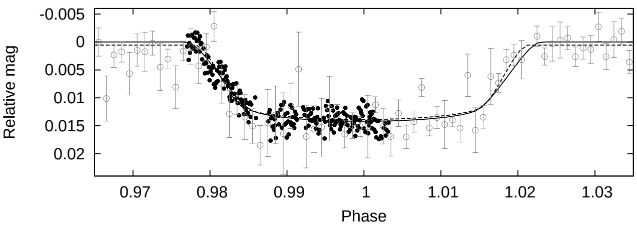

Fig. 4. TRAPPIST partial transit of WASP-79b. The solid-line is the non-main-sequence constrained solution. The dashed-line is that with the main-sequence constraint applied. The offset between the two fits reflects the zero-point rescaling undertaken during the MCMC fits. The WASP photometry is shown as grey circles with errorbars giving the standard deviation within the 0.001 phase bins.

7. Discussion

WASP-78b and WASP-79b are two Jupiter-mass exoplanets transiting the F-type host stars. They occupy the region in parameter space of large radius, low density, exoplanets. The high planetary equilibrium temperature ($T_{\rm P}$ = 2350 ± 80 K) for WASP-78b, makes this one of the hottest exoplanets currently known (Fig. 5), exceeded only by WASP-33b (Collier Cameron et al. 2010), WASP-12b (Hebb et al. 2009) and WASP-18b (Hellier et al. 2009). The mass, radius and density of WASP-78b, are similar to those of HAT-P-32b (Hartman et al. 2011, their circular orbit solution), OGLE-TR-10b (Konacki et al. 2005) and TrES-4b (Chan et al. 2011). Although, similar in radius, WASP-12b is a much denser, more massive planet (Hebb et al. 2009). The large planetary radius of WASP-79b could even exceed that of WASP-17b (Anderson et al. 2010, 2011). However, due to its higher mass, WASP-79b's density is somewhat higher. The main-sequence constrained solution for WASP-79b is, on the other hand, somewhat similar to circular orbit parameters for HAT-P-33b (Hartman et al. 2011).

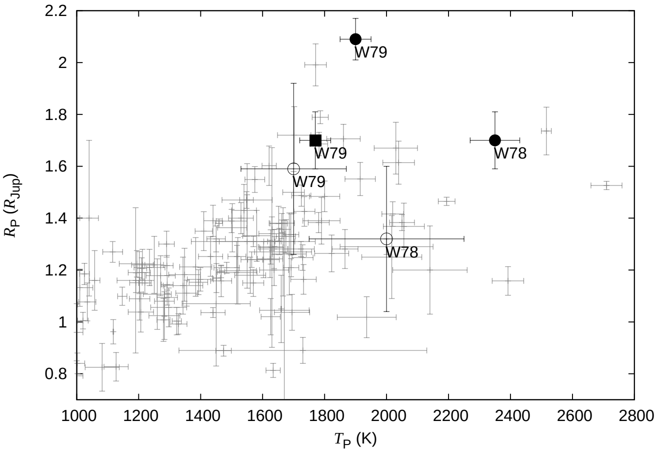

Fig. 5. Location of WASP-78b and WASP-79b in the exoplanet equilibrium temperature–radius diagram. The filled-circles are the non-main sequence constrained parameters, while the filled-square gives the main-sequence constrained parameters for WASP-79b. The open circles shows the values obtained using the stellar radii inferred from the spectroscopic log *g* values (See text for discussion). Values for other exoplanets were taken from TEPCAT (Southworth 2009).

The planetary radius and equilibrium temperature are dependant on the inferred stellar radius. Referring back to the spectral analysis results (Table 2) and using the stellar radii obtained from the Torres et al. (2010) relationships, yields planetary radii of $R_{\rm P}$ = 1.32 ± 0.28 $R_{\rm Jup}$ and 1.59 ± 0.33 $R_{\rm Jup}$ for WASP-78b and WASP-79b, respectively. Both are smaller than those obtained from the transit lightcurves, especially WASP-78b which is slightly over 1-σ away from that obtained from the transit analysis. The equilibrium temperatures for both planets would fall to 2000 ± 250 K and 1700 ± 170 K, respectively. Of course, these results are dependent on the rather imprecise spectroscopic log *g* values, where a relatively small change can have a dramatic effect on the inferred stellar radius.

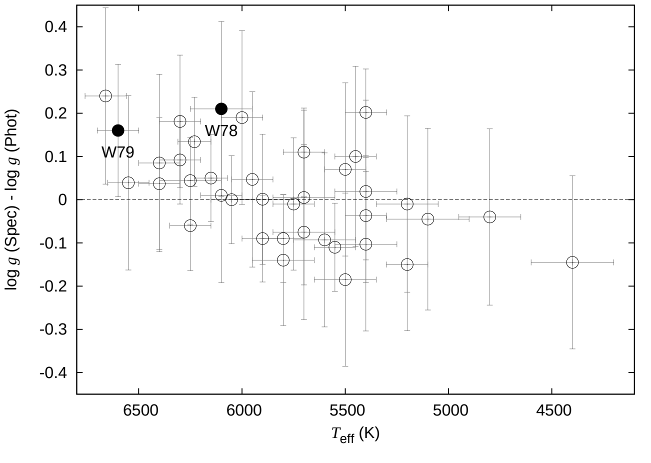

Fig. 6. Difference between spectroscopic log *g* determined from CORALIE spectra for WASP hosts stars and that obtained from transit photometry, as a function of stellar effective temperature ($T_{\rm eff}$).

Table 4. System parameters for WASP-79b. Two solutions are presented: column 2 gives that using the main-sequence constraint, while column 3 give that without this constraint.

Parameter	Value (ms)	Value (no-ms)
Transit epoch (HJD, UTC), T_0	2455545.23479 ± 0.00125	2455545.23530 ± 0.00150
Orbital period, P	3.6623817 ± 0.0000051 d	3.6623866 ± 0.0000085 d
Transit duration, T_{14}	0.1563 ± 0.0031 d	0.1661 ± 0.0037 d
Transit depth, $(R_P/R_*)^2$	0.01148 ± 0.00051	0.01268 ± 0.00063
Impact parameter, b	0.570 ± 0.052	0.706 ± 0.031
Stellar reflex velocity, K_1	0.0882 ± 0.0078 km s^{-1}	0.0885 ± 0.0077 km s^{-1}
Centre-of-mass velocity at time T_0, γ	4.9875 ± 0.0004 km s^{-1}	4.9875 ± 0.0004 km s^{-1}
Orbital separation, a	0.0539 ± 0.0009 AU	0.0535 ± 0.0008 AU
Orbital inclination, i	85.4 ± 0.6 °	83.3 ± 0.5 °
Orbital eccentricity, e	0.0 (assumed)	0.0 (assumed)
Stellar density, $\rho_\star$	0.36 ± 0.04 $\rho_\odot$	0.22 ± 0.03 $\rho_\odot$
Stellar mass, $M_\star$	1.56 ± 0.09 $M_\odot$	1.52 ± 0.07 $M_\odot$
Stellar radius, $R_\star$	1.64 ± 0.08 $R_\odot$	1.91 ± 0.09 $R_\odot$
Stellar surface gravity, $\log g_\star$	4.20 ± 0.03	4.06 ± 0.03
Planet mass, M_P	0.90 ± 0.09 $M_{\rm Jup}$	0.90 ± 0.08 $M_{\rm Jup}$
Planet radius, R_P	1.70 ± 0.11 $R_{\rm Jup}$	2.09 ± 0.14 $R_{\rm Jup}$
Planet surface gravity, $\log g_P$	2.85 ± 0.06	2.67 ± 0.06
Planet density, ρ_P	0.18 ± 0.04 $\rho_{\rm Jup}$	0.10 ± 0.02 $\rho_{\rm Jup}$
Planet equilibrium temperature, T_P	1770 ± 50 K	1900 ± 50 K

Notes. The planet equilibrium temperature, T_P, assumes a Bond albedo of $A = 0$ and even redistribution of heat around the planet. Limb-darkening coefficients for the ms solution were for WASP $a1 = 0.441$, $a2 = 0.599$, $a3 = -0.514$ and $a4 = 0.150$ and TRAPPIST (z') $a1 = 0.517$, $a2 = 0.202$, $a3 = -0.181$ and $a4 = 0.025$, while for the non-ms solution they were for WASP $a1 = 0.447$, $a2 = 0.566$, $a3 = -0.459$ and $a4 = 0.126$ and TRAPPIST (z') $a1 = 0.523$, $a2 = 0.172$, $a3 = -0.133$ and $a4 = 0.004$.

The surface gravities implied by the transit fits for both WASP-78 and WASP-79 are lower than those found from the spectroscopic analyses. Spectroscopic $\log g$ determinations have a typical uncertainty of 0.2 dex (Smalley 2005) and are less precise than those determined from planetary transit modelling. In order to evaluate whether there are any systematic differences, we have compared the spectroscopic $\log g$ values obtained in previous CORALIE analyses of WASP planet-host stars with the values determined using transit photometry (Fig. 6). There is a large scatter in the differences, due to uncertainties in the spectroscopic values, but there does not appear to be any significant systematic difference. There is a hint that the difference may increase for the hottest stars, which could be due to systematic N-LTE effects in the spectroscopic values. In fact, Bruntt et al. (2012) found a similar result from their spectroscopic analyses of stars with asteroseismic $\log g$ values obtained using *Kepler*.

The relatively large difference in $\log g$ from spectroscopy and transit photometry for WASP-78 is probably due to the low S/N of the CORALIE spectrum, where the effects of scattered light and uncertainties in continuum location can result in slight systematics. The $T_{\rm eff}$ values obtained from CORALIE spectra have been found to be in agreement with those from the infrared flux method (Maxted et al. 2011), suggesting that a change of more than 100 K is unlikely. However, Doyle et al. (2012) found that [Fe/H] obtained using CORALIE spectra is, on average, 0.08 ± 0.05 dex lower than found using higher S/N HARPS spectra. Hence, a modest decrease in $T_{\rm eff}$ and/or increase in [Fe/H] could reduce, or even eliminate, the $\log g$ discrepancy. A high S/N spectrum is required to improve the precision of the spectroscopic parameters. In the case of WASP-79, the spectroscopic $\log g$ value could be too high by of the order 0.1 dex due to N-LTE effects. A value of $\log g = 4.1 \pm 0.15$, would give a stellar radius of 1.76 ± 0.37, and a planetary radius of 1.83 ± 0.39 $R_{\rm Jup}$ for WASP-79b. This is now close to the non-main sequence constrained $\log g$ of 4.06±0.03, suggesting that the system parameters are closer to this solution. However, given that the photometry cannot constrain the transit shape, the planetary radius may not be as extreme as 2.09 ± 0.14 $R_{\rm Jup}$. Thus, we conclude that the planetary radius is at least 1.70 ± 0.11 $R_{\rm Jup}$, but possibly somewhat larger. Further transit photometry is required to confirm the planetary parameters.

The empirical relationship for Jupiter-mass exoplanets of Enoch et al. (2012, Eq. 9), predicts planetary radii of 1.78 and 1.56 (1.66 for non-main-sequence solution) for WASP-78b and WASP-79b, respectively. These are in good agreement with that found for WASP-78b, but somewhat smaller than found for WASP-79b (in either of the two cases presented). Enoch et al. (2012) noted that their relationship also significantly underestimated the radius of HAT-P-32b, suggesting that tidal heating could explain the extra inflation, over and above that from stellar irradiation. However, Enoch et al. (2012) used the eccentric solution from Hartman et al. (2011) which Anderson et al. (2012) concluded this is likely to be incorrect and the circular solution should be adopted. This makes HAT-P-32b slightly less bloated, but still larger than given by the empirical relationship. The radial velocities presented here do not preclude the presence of modest eccentricity in either or both of the WASP-78 and WASP-79 systems. Further observations of these two systems are required to fully constrain their properties.

Acknowledgements

WASP-South is hosted by the South African Astronomical Observatory and their support and assistance is gratefully acknowledged. TRAPPIST is a project funded by the Belgian Fund for Scientific Research (Fond National de la Recherche Scientifique, F.R.S-FNRS) under grant FRFC 2.5.594.09.F, with the participation of the Swiss National Science Fundation (SNF). M. Gillon and E. Jehin are FNRS Research Associates. M. Gillon also acknowledges support from the Belgian Science Policy Office in the form of a Return Grant. This research has made use of the SIMBAD database, operated at CDS, Strasbourg, France.

References

Anderson, D.R., Hellier, C., Gillon, M., et al. 2010, ApJ, 709, 159
Anderson, D.R., Smith, A.M.S., Lanotte, A.A., et al. 2011, MNRAS, 416, 2108
Anderson, D. R., Collier Cameron, A., Gillon, M., et al. 2012, MNRAS, 422, 1988
Arras, P., & Socrates, A. 2010, ApJ, 714, 1
Baranne, A., Queloz, D., Mayor, M., et al. 1996, A&AS, 119, 373
Barnes, S.A. 2007, ApJ, 669, 1167
Batygin, K., & Stevenson, D. J. 2010, ApJ, 714, L238
Boesgaard, A. M., & Tripicco, M. J. 1986, ApJ, 302, L49
Böhm-Vitense, E. 2004, AJ, 128, 2435
Bruntt, H., Deleuil, M., Fridlund, M., et al. 2010, A&A, 519, A51
Bruntt H., Bedding T.R., Quirion P.-O., et al., 2010, MNRAS, 405, 1907
Bruntt, H., Basu, S., Smalley, B., et al. 2012, MNRAS, 423, 122
Chan, T., Ingemyr, M., Winn, J. N., et al. 2011, AJ, 141, 179
Charbonneau, D., Brown, T. M., Latham, D. W., & Mayor, M. 2000, ApJ, 529, L45
Charbonneau, D., Allen, L.E., Megeath, S.T., Torres, G., & Alonso, R. 2005, ApJ, 626, 523
Claret, A., 2000, A&A, 363, 1081
Collier Cameron, A., Pollacco, D.L., Street, R.A., et al. 2006, MNRAS, 373, 799
Collier Cameron, A., Wilson, D.M., West, R.G., et al. 2007, MNRAS, 380, 1230
Collier Cameron, A., Guenther, E., Smalley, B., et al. 2010, MNRAS, 407, 507
Enoch, B., Collier Cameron, A., & Horne, K. 2012, A&A, 540, A99
Doyle, A. P., Smalley, B., Maxted, P. F. L., et al. 2012, MNRAS, submitted.
Fortney, J. J., Marley, M. S., & Barnes, J. W. 2007, ApJ, 659, 1661
Fortney, J. J., Demory, B.-O., Désert, J.-M., et al. 2011, ApJS, 197, 9
Fortney, J. J., & Nettelmann, N. 2010, Space Sci. Rev., 152, 423
Gillon, M., Smalley, B., Hebb, L., et al. 2009, A&A, 496, 259
Gillon, M., Jehin, E., Magain, P., et al. 2011, Detection and Dynamics of Transiting Exoplanets, St. Michel l'Observatoire, France, Edited by F. Bouchy; R. Díaz; C. Moutou; EPJ Web of Conferences, Volume 11, id.06002, 11, 6002
Gillon, M., Doyle, A. P., Lendl, M., et al. 2011, A&A, 533, A88
Gray, D.F., 2008, The observation and analysis of stellar photospheres, 3rd Edition (Cambridge University Press), p. 507.
Hartman, J. D., Bakos, G. Á., Torres, G., et al. 2011, ApJ, 742, 59
Hebb, L., Collier-Cameron, A., Loeillet, B., et al. 2009, ApJ, 693, 1920
Hellier, C., Anderson, D. R., Collier Cameron, A., et al. 2009, Nature, 460, 1098
Jackson, J., & Stoy, R. H. 1954, Annals of the Cape Observatory, 17A
Jehin, E., Gillon, M., Queloz, D., et al. 2011, The Messenger, 145, 2
Jones, D.H., Read, M.A., Saunders, W., et al. 2009, MNRAS, 399, 683
Konacki, M., Torres, G., Sasselov, D. D., & Jha, S. 2005, ApJ, 624, 372
Latham, D. W., Borucki, W. J., Koch, D. G., et al. 2010, ApJ, 713, L140
Lucy, L.B., & Sweeney, M.A. 1971, AJ, 76, 544
Magain, P. 1984, A&A, 134, 189
Maxted, P. F. L., Koen, C., & Smalley, B. 2011, MNRAS, 418, 1039
Mayor, M., & Queloz, D. 1995, Nature, 378, 355
Pepe, F., Mayor, M., Galland, F., et al. 2002, A&A, 388, 632
Perna, R., Menou, K., & Rauscher, E. 2010, ApJ, 724, 313
Pollacco, D.L., Skillen, I., Collier Cameron, A., et al. 2006, PASP, 118, 1407
Pollacco, D.L., Skillen, I., Collier Cameron, A., et al. 2008, MNRAS, 385, 1576
Queloz, D., Mayor, M., Weber, L., et al. 2000, A&A, 354, 99
Queloz, D., Henry, G.W., Sivan, J.P., et al. 2001, A&A, 379, 279
Sestito, P., & Randich, S., 2005 A&A, 442, 615
Smalley, B. 2005, Mem. Soc. Astron. Ital. Suppl., 8, 130
Southworth, J. 2009, MNRAS, 394, 272
Southworth, J. 2011, MNRAS, 417, 2166
Torres, G., Andersen, J. & Giménez, A, 2010a, A&A Rev., 18, 67
Winn, J.N., 2009, IAU Symposium, 253, 99